Demonstration of real-time event camera to collaborative robot communication

Analysis of bend-over gesture wearing a trunk-support exoskeleton

Mattia Antonelli[1], Michele Polito[1], Stefano Pastorelli[1] and Laura Gastaldi[1]

[1] Dept. of Mechanical and Aerospace Engineering, Politecnico di Torino, Turin, Italy
Mattia.antonelli@polito.it

Abstract. In the context of industrial tasks, back exoskeletons aim at reducing operator's muscular effort during the work gesture and prevent professional illnesses. Passive devices have the limitation of providing fixed support based on a single angle of bending kinematics. In this study, a multibody model previously validated was used to evaluate the biomechanical effects of assistance provided by passive exoskeletons in terms of joint actions. Specifically, the model, which involves the DOF allowed by the spine in the waist joint, reproduced experimental kinematics of two subjects realizing stoops and squats at various speeds. Kinematics was measured using an active exoskeleton prototype developed by the authors and inertial sensors (IMUs). Simulations revealed that passive assistance results in joint internal reactions mainly along the sagittal axis, which may lead to discomfort and instability in squat bending. Results underscore the importance of developing flexible laws for active systems able to adjust support dynamically to users' movements and preferences.

Keywords: Wearable Robotics, trunk-support exoskeleton, biomechanical model, bend-over strategy, lifting strategy.

1 Introduction

Despite the new paradigm of robots at the service of industry aiming to achieve performance excellence, many workers continue to face physical exertion in tasks where human skills and flexibility cannot be replaced [1, 2]. Physical strains can cause work-related musculoskeletal disorders (WMSDs), particularly affecting back muscles in repetitive and prolonged activities [3]. Among wearable assistive technology, exoskeletons aim to safeguard workers' health, by reducing muscular workload and exposure to occupational disease [4, 5]. Manufacturers and researchers have analyzed various architectures and functionalities of exoskeletons designed for specific industrial tasks, exploring both passive and active solutions [6, 7].

Passive exoskeletons incorporate mechanical elements like springs or elastic bands, which can store and release energy, with an a priori predetermined law. For this reason, passive devices cannot adapt to the variability of worker’s behaviors who can adopt various techniques during material handling and bend-over, exploring different kinematic ranges of human joints and also involving secondary movements like standing, walking and sitting [8]. The support released by passive exoskeletons neglects differences between users and their kinematics [9]. Thus, despite their simplicity, weight and

cost advantages, the lack of support law modularity results in user discomfort and instability perception, making them unsuitable for certain industrial tasks. On the contrary, active devices offer flexible and adaptive assistance, adjusting it according to the wearer's kinematics, comfort, and perceptions. The challenge in implementing an active exoskeleton involves developing control laws that can adapt to personal support preferences and movement variability.

To objectively investigate the validity of an assistance strategy, it is necessary to evaluate the biomechanical effects on the user's joints. Since musculoskeletal loads cannot be easily measured experimentally, human multibody modelling has been exploited to simulate industrial tasks. Van del Have et al. developed an OpenSim model, evaluating joint torques and peak power during lifting movements [10]. Multibody simulations were exploited also to assess an upper-exoskeleton assistive effect [11], evaluate a new device design concept [12] and investigate the whole-body control of a lower limb exoskeleton [13]. However, many studies involving multibody modelling during bend-over movements typically connect the trunk and thighs by the hip joints, neglecting the range of motion permitted by the spinal column. It, together with the hip joint, allows differentiating among bend-over techniques. The Simscape human model proposed in [14] and optimized in this study approximates the degree of freedom (DOF) allowed by the spinal column concentrating it in the vertebrae L5-S1 as a single joint defined waist. Hence, the back flexion-extension is modelled as the interaction of three links (thigh, pelvis, and trunk) and two joints (waist and hip).

The study goal is to exploit the multibody model to design and assess assistance strategies in terms of joint torque and reaction forces considering the varying kinematics among bend-over techniques. The embedded sensor system of a powered exoskeleton prototype, implemented by the authors and detailed in [15], and additional inertial sensor units (IMUs) were used to collect kinematic data from two subjects while performing stoops and squats. The captured joint angle kinematics were exploited in the multibody model to simulate the effect of a passive support strategy, aiming to assess its limitations concerning comfort perception and adaptability to movement.

2 Material and Methods

2.1 Exoskeleton prototype

An active exoskeleton prototype was implemented by the authors to assist the wearer’s trunk during industrial lifting, static bending, and posture maintenance, according to user preference and kinematic configuration [15]. However, in this study, the exoskeleton was exploited to gather experimental kinematic data from two subjects performing different bending movements while wearing the device, as depicted in Fig. 1.

The prototype consists of a main central structure and two interaction parts on the chest and legs. The former comprises two pelvic plates connected by a pelvic belt, that include active electric joints aligned with the hips, as illustrated in Fig.1a. Each active joint is coupled with the pelvis plate through a bushing to allow free rotation. A chest interface is linked laterally to the joints via rigid bars called trunk supports and

posteriorly to the pelvic belt using fabric belts. Additionally, two pads are attached to the thighs and connected to the active joints by two rigid segments, named leg supports.

The design of the active joint, detailed in [15], enables torques up to 65 Nm for each side. Each active joint can measure the angle between the trunk and leg supports through an encoder integrated into the motor and provide a torque between them, exchanging support forces at the user's chest and thighs to reduce the joint load and muscle efforts. Moreover, an angular sensor system embedded in each joint enables the user's kinematics tracking, allowing differentiation among the various bending strategies and offering adaptable support. Other prototypes use an additional IMU for measuring trunk inclination and a hip kinematic sensor and adapt support [16, 17]. This device integrates sensors directly into the structure, avoiding external sensors that can introduce errors (e.g. inclined floor) and extend dressing times, unsuitable for industrial settings.

The control system, communication, and sensor acquisition are implemented remotely on a PC using LabVIEW (National Instruments®, USA) operating at 50 Hz.

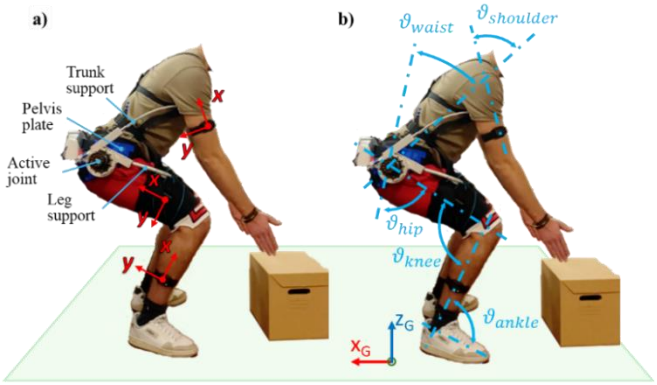

Fig. 1. User performing a bend-over while wearing the active prototype: a) device main components, IMUs reference frames and placement on human segments; b) Joint angles in a generic configuration.

2.2 Motion capture procedure and signal processing

Two male subjects were recruited for the study, both with a height of 1.80 m and body mass 73 kg and 65 kg respectively. Each participant maintained an initial standing reference configuration for 10 seconds, then executed 5 stoops and 5 squats suggested in random order on a screen every 15 seconds. The bending movements were performed lifting an empty box for each of three self-selected speeds (slow, normal, fast) while wearing the active exoskeleton. Since in the study the active prototype is exploited only for its kinematic measuring function, it was controlled through the *transparency mode* [15], allowing users to perceive no obstruction and perform unrestricted movements. Transparency setting was calibrated according to user's comfort.

The angular sensor system enables tracking the angular displacement between the trunk support and leg support, as well as the angle variation between the leg support and the pelvic plate. These values are measured as the difference of a generic configuration with respect to the initial neutral posture. By combining these measurements, the

hip and waist joint angles, named ϑ_{hip} and ϑ_{waist} respectively, can be estimated, as indicated in Fig.1b for a generic posture. Additionally, the embedded sensor system allows the evaluation of the angular velocities $\dot{\vartheta}_{hip}$ and $\dot{\vartheta}_{waist}$.

To capture the full-body kinematics during the trials, three IMUs were placed on the subjects' right shank, right thigh, and right upper arm following the standardized manual unit-to-body segment alignment (Fig. 1a). Angular kinematics was recorded at a frequency of 100 Hz. Movements were assumed to be symmetrical with respect to the sagittal plane and only kinematics from the right side was considered. This was confirmed by observing a mean variation below 2 degrees and a maximum peak variation of 15% between the ϑ_{hip} angles of the right and the left side during all the trials. Ankle joint kinematics is derived by assuming that the foot remains constantly attached to the ground. Specifically, the ankle angle ϑ_{ankle} is determined by assessing the relative orientation of the shank IMU during the whole trial and its averaged orientation during the 10-second static reference posture maintenance. Then, the knee joint angle ϑ_{knee} was evaluated decomposing the orientation of the distal IMU on the shank expressed respect to the proximal IMU on the thigh after referring both to the initial reference posture. Shoulder angle $\vartheta_{shoulder}$ was calculated using the relative orientation of the IMU on the upper arm referred to the IMU on the thigh and considering ϑ_{hip} and ϑ_{waist}. Similarly, ankle, knee and shoulder angular velocities and accelerations were calculated from IMU data. Instead, $\dot{\vartheta}_{hip}$ and $\dot{\vartheta}_{waist}$ from device sensors were derived and filtered obtaining accelerations. Signal filtering was conducted using a low-pass 2nd-order Butterworth filter with a cutoff frequency of 5 Hz. Synchronization between signals from the two capture systems was achieved using a trigger signal emitted by the IMUs station and received by the device acquisition board. Following synchronization, joint kinematics was segmented and collected based on bending type and motion speed. The repeatability of kinematic signals with the same speed and within the same bending techniques was evaluated with Pearson correlation coefficient r^2 achieving values above 0.9 for all the movements. Signals of each simulation were aligned in time and then averaged according to the bending strategy and execution speed to obtain an average trend and dispersion. Custom MATLAB 2023b© routines were developed to execute the signal processing and Simulink© environment was chosen to implement the simulations.

2.3 Human multibody model

The multibody model developed and validated in a previous study [14] using MATLAB Simscape Multibody software (MATLAB©, USA) has been updated for this analysis.

It consists of 15 rigid bodies connected by 14 joints, with each joint modelled as three revolute joints in series, except for the knee and elbow joints, which have only one revolute joint. The model includes two lower limbs composed of the foot, shank, and thigh linked by ankle and knee joints. Additionally, the model introduces the waist joint to divide the back into trunk and pelvis considering the contribution of waist and hip joint flexions during different bend-over techniques. The hip joint links the pelvis to the thigh. Finally, two shoulder joints connect the trunk to the upper limbs (hand, forearm, and upper arm, linked by wrist and elbow joints). The foot is anchored to the

ground using a rigid transformation. The device assistance is modelled by applying forces at its contact points with the body. This involves applying two forces perpendicular to the trunk and thigh bodies respectively at chest and mid-thigh levels and one force applied to the hip joint as the vector sum of the previous ones. In this study, the model does not incorporate the weight of the device during simulation.

2.4 Simulation

To implement the simulation, the model body segments are proportionally scaled based on the subject's anthropometric data: mass, height, and trunk and limb lengths.

Experimental joint kinematics recorded during stoops and squats were used as input for the multibody model. Specifically, kinematics obtained from the IMUs were assigned to the model ankle, knee, and shoulder joints, while the hip and waist joints received input from the exoskeleton data. Since movements occur mainly within the sagittal plane, null kinematics was imposed along the other two axes during the simulation. The MATLAB solver was selected as variable-step ode45. Simulation outputs are the net human hip and waist torques and reaction forces applied from the proximal body to the distal one, evaluated through inverse dynamics.

Initially, simulations on the experimental bending kinematics were performed without integrating exoskeleton assistance. This aimed to explore variations in joint torques depending on the subjects and the postures adopted during different bending techniques performed at various speeds, as well as a benchmark for assessing the effectiveness of the support strategy. Subsequently, the conventional support offered by passive systems, which rely solely on the variation of the angle between the interaction points (the angle between trunk and leg supports in this device), was designed and compared with non-assisted dynamics. The support torque is proportional to the relative angular displacement between thigh and trunk segments, regardless of the bend-over technique. The design point that defines the exoskeleton stiffness k concerns a torque peak value provided by the device equal to 70 Nm when this relative angle variation reaches 101 degrees (maximum value recorded during experimental tests), defining k as 0.69 Nm/deg. This torque value contributes to a 50% reduction of peak torque generated by the hip joint at the bending maximum flexion angle [18]. The magnitudes of assistive forces applied to the chest and thigh during the simulation were calculated by dividing the torque by the distances between each application point and the hip joint.

3 Results

Changes in joint actions were examined to understand whether the biomechanical effects of passive assistance were acceptable. Only graphs for subject 2 considering stoop and squat at slow speed are presented, as both subjects yielded similar outcomes.
Fig. 3 presents a comparison between the hip joint torques with and without the passive assistance law, considered as the sum of both hip contributions. The graphs in the first row depict trends during stoops on the left and squats on the right. In the second row, passive assistive torque profiles are illustrated according to the bending technique.

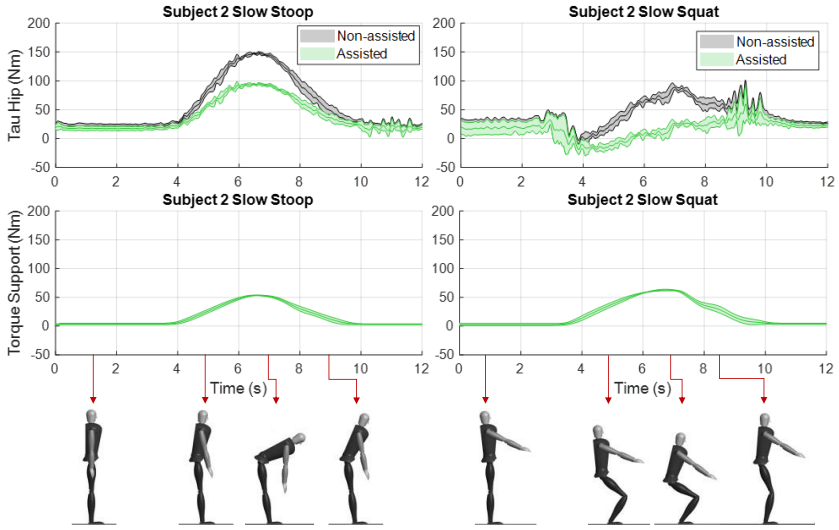

Fig. 3. Hip joint torques comparison between assisted (green) and non-assisted (grey) cases (first row) and assistive torques profiles (second row) during stoops (left) and squats (right) for subject 2.

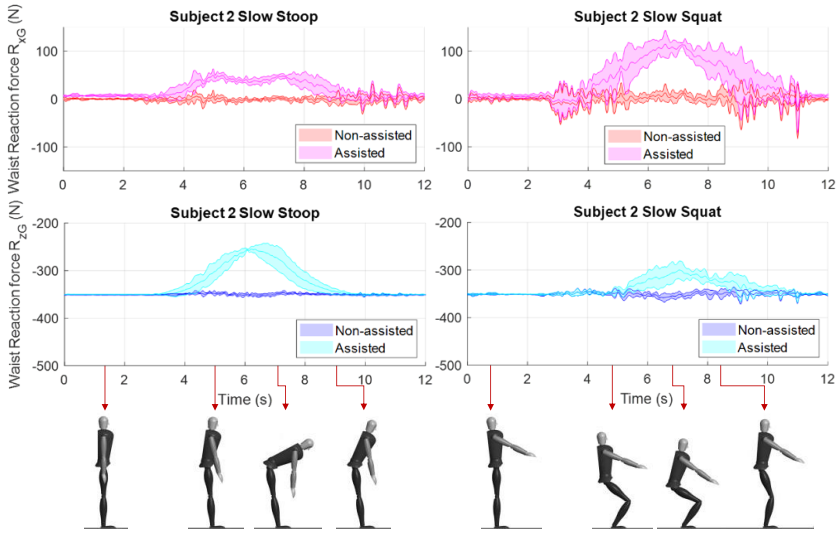

Fig. 4. Waist reaction forces during stoops (left) and squats (right) for subject 2. R_x trends are shown in the top row, with the assisted case in magenta and the non-assisted case in red. R_z trends are displayed in the bottom row, with the assisted case in cyan and the non-assisted case in blue.

Postures assumed during the two different bending techniques are depicted at the bottom to show the technique differences on the kinematic chain. Assistance is determined by the relative angle between the thigh and trunk, which exhibits similar profiles across both techniques as indicated by torque trends, despite different model postures

reported for stoops and squats. Both stoops and squats exhibit a reduction in hip torques when supported with the passive strategy compared to non-assisted motion, as well as in the waist. All graphs correspond to trials conducted at a slow self-selected velocity. Trends in normal and fast speed trials report similar shapes, with increased peak torques and more pronounced variations due to inertial effects.

Figure 4 evaluates the passive assistance in terms of waist reaction forces along the ground x-axis and z-axis, with R_{xG} shown above and R_{zG} below. Force outputs were referred to the ground coordinate system depicted in Fig. 1, which aligns with the body anatomical sagittal, transversal, and longitudinal axes. Expressing the reaction forces along these directions allows the evaluation of their magnitudes and direction effects on the body in terms of imbalance and instability with greater clarity. Trends during stoops (left column) and squats (right column) are depicted, comparing the assisted and non-assisted motions. A reduction in R_{zG} and an increase in R_{xG} can be observed in the assisted to non-assisted movements comparison. Similar outcomes characterize the hip joint forces, while knee and ankle joints do not present any torque and force differences between the assisted and non-assisted cases, across both subjects and execution speeds.

4 Discussion

Passive assistance reduces the torque required to the user's hip joint to perform both stoops and squats, especially during the phase of maximum flexion. Reductions of up to 60 Nm are observed. Focusing on squat, the torque exhibits a trend opposite to the flexion direction in the first motion instants resulting in negative values, which is further exacerbated by the assistance. In the remaining part of the movement, the assistance almost nullifies the user moment. The trend of the assistive torque is similar between stoop and squat, but subjects should not receive the same support in both situations since they assume different postures. However, observing only hip torques it is not possible to infer evidence of unsuitability and discomfort caused by this passive support, as it appears to alleviate effort for both subjects.

Similarly, the passive law provides support by reducing the reaction force R_z at the waist and hip during both stoops and squats. This is achieved as the device applies action against the chest and thighs, thereby reducing the workload on the joints along the vertical axis. However, along the x-axis, the user undergoes a reaction force when assisted which is not present in non-assisted simulations. During stoops, this force barely reaches 50 N, but during squats, it peaks at up to 150 N, also increasing in trials with normal and fast speeds. During squats, this force exerted backwards on the user leads to instability and contributes to the discomfort experienced by the wearer while aided by a passive device. Passive assistance based on the angle between the trunk and thighs does not consider the techniques employed by the operator, as the angle exhibits a similar range in both stoops and squats. Assisting all bend-over techniques equally leads to discomfort, reducing device adoption and acceptability among workers. Active devices can be exploited to assist the different bending techniques in specific ways. Achieving this requires the development of a technique identification algorithm based on sensor kinematic measurements which modulates the support. Assistance tailored to

the bending technique will avoid instability and discomfort perceived by the user when adopting a passive device during squat movements. The main limitation of this study is the small sample size analyzed. Future work includes expanding the sample, assessing active strategies, and validating through muscle effort evaluation.

5 References

1. Tsarouchi P, Makris S, Chryssolouris G: Human-robot interaction review and challenges on task planning and programming. Int J Comput Integr Manuf 29:916–931 (2016)
2. McDevitt S, Hernandez H, Hicks J, et al: Wearables for Biomechanical Performance Optimization and Risk Assessment in Industrial and Sports Applications. Bioengineering 9 (2022)
3. Jan de Kok, et al: Work-related musculoskeletal disorders prevalence, costs and demographics in the EU. European Health (2019)
4. Bär M, et al: The influence of using exoskeletons during occupational tasks on acute physical stress and strain compared to no exoskeleton – A systematic review and meta-analysis. Appl Ergon 94 (2021)
5. Kermavnar T, et al.: Effects of industrial back-support exoskeletons on body loading and user experience: an updated systematic review. Ergonomics 64:685–711 (2021)
6. Spada, S., et al: Passive Upper Limb Exoskeletons: An Experimental Campaign with Workers. Advances in Intelligent Systems and Computing, 825, pp. 230–239 (2019)
7. Hyun DJ et al: Singular Wire-Driven Series Elastic Actuation with Force Control for a Waist Assistive Exoskeleton, H-WEXv2. IEEE/ASME Transactions on Mechatronics 25:1026–1035 (2020)
8. Del Vecchio L: Choosing a Lifting Posture: Squat, Semi-Squat or Stoop. MOJ Yoga & Physical Therapy 2 (2017)
9. Ali A, Fontanari V, Schmoelz W, Agrawal SK: Systematic Review of Back-Support Exoskeletons and Soft Robotic Suits. Front Bioeng Biotechnol 9 (2021)
10. van der Have A, Van Rossom S, Jonkers I: Squat lifting imposes higher peak joint and muscle loading compared to stoop lifting. Applied Sciences (Switzerland) 9 (2019)
11. Gull MA, Bak T, Bai S: Dynamic modeling of an upper limb hybrid exoskeleton for simulations of load-lifting assistance. Proc Inst Mech Eng C J Mech Eng Sci 236:2147–2160 (2022)
12. Harant M, Näf MB, Mombaur K: Multibody dynamics and optimal control for optimizing spinal exoskeleton design and support. Multibody Syst Dyn 57:389–411 (2023)
13. Kang J, Kim D, Chung HJ, et al: Whole-body Control Based Lifting Assistance Simulation for Exoskeletons. Int J Control Autom Syst 21:1950–1958 (2023)
14. Panero E, et al: Influence of hinge positioning on human joint torque in industrial trunk exoskeleton. Mechanisms and Machine Science 73:133–142 (2019)
15. Antonelli M, et al: Experimental Characterization of Active Joint for Trunk Exoskeleton. In: Advances in Italian Mechanism Science. IFToMM Italy 2022. Mechanisms and Machine Science. pp 593–600 (2022)
16. Lanotte F, et al: Adaptive Control Method for Dynamic Synchronization of Wearable Robotic Assistance to Discrete Movements: Validation for Use Case of Lifting Tasks. IEEE TRANSACTIONS ON ROBOTICS 37 (2021)
17. Huang S, et al: Biomechanical Design and Evaluation of a Lightweight Back Exoskeleton for Repetitive Lifting Tasks. In: Lecture Notes in Computer Science. Springer Science and Business Media Deutschland GmbH, pp 475–488 (2023)
18. Hwang S, Kim Y, Kim Y: Lower extremity joint kinetics and lumbar curvature during squat and stoop lifting. BMC Musculoskelet Disord 10 (2009)